Characterization of a Fast Response Fiber-Optic pH Sensor and illustration in a Biological Application

Jan Werner,*[ab] Mathias Belz,[cd] Karl-Friedrich Klein,[b] Tong Sun[a] and K.T.V. Grattan[a]

Optical, and especially fiber-optic techniques for the sensing of pH have become very attractive and considerable research progress in this field has been made over recent years. The determination of the value of pH across a broad range of applications today, important for areas of study such as life sciences, environmental monitoring, manufacturing industry and widely in biologically research is now accessible from such optical sensors. The need for such technology arises because familiar, commercial sensors are often limited in terms of their response time and the presence of drift, all of which emphasize the value of newer and rapidly developing technologies such as fiber-optic sensors, to address these wider applications. As a result, a new compact sensor design has been developed, designed around a specially-formed fiber-optic tip, coated with a pH-sensitive dye, and importantly covalently linked to a hydrogel matrix to provide high stability. The sensor developed was designed to have a very fast response time (to 90% of saturation, Δt_{90}) of < 5 s and a sensing uncertainty of ~± 0.04 pH units. Given the covalently bonded nature of the dye, the problem of leaching of the indicator dye is reduced, creating a probe which has been shown to be very stable over many days of use. Illustrating this through extended continuous use, over ~12h at pH 7, this stability was confirmed showing a drift of < 0.05 pH/h. In order to give an illustration of the value of the probe in an important biological application, the monitoring of pH levels between pH 7 to pH 8 in an AMES' medium, a substance which is important to maintain the metabolism of retinal cells is shown and the results as well as temperature stability of the probe discussed.

Introduction

The determination of the pH level is very important across a broad range of applications today: in life sciences, environmental monitoring, biomedical research and widely in industry globally, as discussed in a recent review of the field[1]. For example, there is particular interest in detecting pH values using optical techniques for areas as diverse as biological studies of tissues[2] and cells[3,4], process control in bioreactors[5–9], seawater analysis[10,11] or even corrosion monitoring[12] – thus it has a key role in biotechnology today. Further, pH measurement is particularly important across a range of important industries internationally, acting as one of the primary indicators of quality. In the multi-billion dollar food industry, monitoring of pH is important in determining the taste and state of preservation of many food products.

Classical pH glass electrodes have been well known and used for the measurement of pH values over many decades. However, these types of sensors show the important disadvantages of often being bulky and their glass surfaces make them fragile and subject to breakage, even when they are handled carefully. Further, the signal obtained can be subject to interference from stray electromagnetic fields, making them unsuitable for use in many situations where measurements are needed. However, there are alternatives – optical, and especially fiber-optic sensors have become very attractive for the wide variety of pH measurements discussed, and undoubtedly needed in the future, since these sensors are usually reversible and easy to miniaturize (< 50µm). Due to the use of small diameter fiber, they can be inexpensive to fabricate and can be employed in situations where the presence of electromagnetic interference would mean that conventional sensors would often fail. Therefore, there is increasing demand for new and better fiber-optic pH sensors of this type, for a wide range of research fields as well as commercial and industrial uses[13] – and this has driven the research program underpinning the industry-academic collaborative work reported here.

Commercial activities in the field have developed significantly in recent years and therefore it is not surprising that since 2000, the commercial success of such sensors has resulted in a growing number of companies manufacturing and selling products in these areas. Illustrative examples from products from different countries globally include PreSens Precision Sensing GmbH (www.presens.de), Ocean Insight Inc. (www.oceaninsight.com), World Precision Instruments Inc. (www.wpiinc.com), PyroScience GmbH (www.pyroscience.com), Unisense (www.unisense.com), Ohio Lumex (www.ohiolumex.com) and many others. Not surprisingly, a large number of the research developments which first were reported in the scientific literature are now reflected in commercially available products, allowing the user to have access to a wide range of different system designs, ranging from large (robust)[10,14–16] to very small[2–4,17,18] – and that can be applied across the broad range of applications where they are needed now.

Although optical fiber sensor systems go back to the 1970s, they have matured in recent years and depending on the sensing methodology chosen, the pH change measured could be as a result of different types of optical interactions, such as absorbance/reflectance, luminescence or for some multiple sensing concepts, a combination of both. In addition, monitoring of refractive index, light scattering and light polarization have also been used as parameters to detect pH changes[2]. However, due to the advantages that they show and as mentioned above, the majority of optical pH sensors that have been developed and are used in biological applications and

indeed are commercially available, are based on indicator dyes that change their optical properties in respect to changes in the pH values of the solutions into which they are placed[1,19–23].

In general, an optical sensor system for pH monitoring using an optical effect to reflect the pH changes occurring requires an indicator dye that changes its wavelength response (or colour), when interacting with solutions of different pH values. Many different dyes display characteristics that are appropriate for such sensors, and examples of widely used dyes are SNARF, SNAFL, HPTS[19,20,22] and several novel NIR indicators[21,24,25] – some now being used in commercial products. Typically, the indicator dye used is held or immobilized in a supporting matrix (e.g. polymers or hydrogels[26]) that needs to be permeable to hydrogen ions. Three widely used methods for the immobilization of a dye in a solid matrix are frequently seen in probe designs that have been reported: adsorption, physically entrapment and covalent binding[22]. Looking at these more closely, covalent binding is usually complex and time-consuming and needs an appropriate material suitable for the immobilization. However, where dyes are used as pH-sensitive materials, covalent binding is often preferred, for example to eliminate the leaching effects[13,22] which are unacceptable in many clinical or biotechnology applications. In a typical fiber-optic sensor design, the pH sensitive material is applied to the fiber tip using a suitable coating procedure. Different methods to do this are available, but amongst these the most popular are dip coating, spin coating or photo-polymerization. Thus the signal change measured could then occur as a result of different types of interactions, these depending on the sensing materials chosen or pH-dependent signal generated (e.g. absorbance/reflectance or luminescence (intensity or lifetime)), seen amongst the most widely used optical techniques used to detect pH values[20–22].

Dual Lifetime Referencing (DLR), where the decay times of two indicators that are immobilized in a polymeric matrix are measured simultaneously[27,28] is a very popular sensing methodology for pH monitoring. Alternatively, methods based on a single luminescence intensity measurement of only one indicator dye[12,29] are possible, this being preferable where reducing the complexity of the sensing chemistry, and thus the detection system, is beneficial. This can be illustrated when considering the reduction in the number of excitation sources and emission detectors needed, thus importantly impacting positively on the overall system cost. Compared to a ratiometric approach such as DLR, direct luminescence measurements have the disadvantage that they can be strongly influenced by problems such as photo-bleaching, stray light entering the detection system and any drift of the electronic components that may occur[20,21]. However, a careful choice of indicator dye, such as one with a relative strong emission intensity and the creation of a "smart" optoelectronic detection system (e.g.: drift-compensated concepts or pulsed light sources) can significantly reduce such effects.

The choice of the sensing element (dye and supporting matrix) and the optical platform (in this case, the fiber tip) where the coating is attached[22,30] will have a major influence on the sensitivity and response time to pH, as well as the detection range and long-term system stability. Optimization of the design of the fiber tip, for example in reducing its size and that of the dye-based coating, has the potential to reduce the response time (but this will have a concomitant effect on signal strength). The choice of optical fiber is important, since its' physical properties significantly influences the light guidance in the optical fiber chosen[31,32] and thus the overall performance of the instrument created.

Looking at what is currently on the market, available luminescence-based pH sensors typically have reported response times (to 90% of saturation, Δt_{90}) from 20 s to an extreme of 50 minutes[2,4,10,12,14–17]. Often, however, shorter response times are needed in practical cases, and in this work the focus has been on the reduction of this parameter (while still maintaining the sensitivity of the device). The fiber-optic pH sensor developed in this research and reported here has been based on innovation in the design through creating a specially formed and chemically-treated tip, allowing an optimization of the light emission from the probe – permitting the use of thinner coatings on the fibre tip itself. This typically will have a positive influence on the sensor performance through allowing faster response times to be achieved than have typically been reported from luminescence-based sensors (for pH monitoring). The tip design created and developed here is one based on an indicator dye, this being selected to be suitable for the physiologically important pH range of pH 5 to pH 8.5, using covalent binding to a hydrogel during a photo-polymerization process. Monitoring the pH value through measuring the pH-induced changes in the luminescence intensity is the method employed, integrating this further into a newly developed instrument. Additionally attention is paid in the design to reducing the effect of photo-bleaching and of the ingress of stray light, performance-limiting problems in many conventional sensors. The sensor created has been shown to be very stable over a long period of time, having a short response time and importantly for biomedical applications in particular, no dye leaching. Finally, the full instrumental system performance has been cross-compared with that from a familiar commercially available fiber-optic instrument and here a preliminary evaluation in an important biological application is discussed.

Material and methods

Principle of pH measurement based on fluorescence intensity

The pH scale was introduced by Søren P. L. Sørensen in 1909 where pH firstly was described as the negative logarithm of the hydrogen ion concentration[33], establishing the principle of pH measurement. pH is defined in terms of hydrogen ion activity a_{H^+} such that:

$$\mathrm{pH} = -\log a_{H^+} \quad (1)$$

Classical electrochemical sensors directly measure the activity of hydrogen ions in aqueous solutions and optical pH sensors the concentrations of the protonated and deprotonated form of the indicator dye. By contrast, the fiber-optic sensor scheme designed and reported in this paper is based on *a fluorometric determination of pH*, where the change in this effect results in a change of the luminescence intensity observed. The well-known Henderson-Hasselbalch equation is commonly used to determine the value of pH from the changes of the deprotonated [A^-] and protonated [HA] form, using an optical signal method[22] as shown below:

$$\mathrm{pH} = \mathrm{pK_a} - \log\frac{[\mathrm{HA}]}{[\mathrm{A^-}]} \quad (2)$$

where pK_a is the acid-base constant of the indicator dye. [A^-] and [HA] are then related to fluorescence intensities observed from the sensor through [A^-] = I_m - I_{min} and [HA] = I_{max} - I_m. The signal I_m is the measured luminescence intensity from the indicator in the sensor system. Defining I_{max} as the maximum luminescence intensity signal of the deprotonated form and I_{min} as the minimum luminescence intensity signal of the protonated form, the value of pH in solution causing that particular change can be calculated by substituting these expressions into Eq. (2), giving:

$$\mathrm{pH} = \mathrm{pK_a} - \mathrm{b} \cdot \log\left(\frac{\mathrm{I_{max}} - \mathrm{I_m}}{\mathrm{I_m} - \mathrm{I_{min}}}\right) \quad (3)$$

where b is the numerical coefficient to determine the slope of the function. Rewriting Eq. (3) in terms of I_m results in the well-known sigmoidal function centered on the pK_a value [34]:

$$\mathrm{I_m} = \mathrm{I_{min}} + \frac{\mathrm{I_{max}} - \mathrm{I_{min}}}{1+10^{-\left(\frac{\mathrm{pH}-\mathrm{pKa}}{\mathrm{b}}\right)}} \quad (4)$$

Fabrication of the fiber-optic pH sensor probe

All chemical used in the work, as well as certified temperature-stable standard buffer solutions (Certipur® Certified Reference Material), were purchased from Merck and used as supplied.
A commercially available 400/430 µm (core/cladding) silica fiber was selected as the basis of the sensor probe and this was purchased from Polymicro Technologies. However, the tip of the fiber was specially formed during a thermal process to decrease the fiber diameter to < 50 µm using a fusion splicer (Fujikura Arc Master FSM-100P+). Figure 1 shows an image of the tip design following the taper forming process, as well as illustrating the intensity distribution when coupling light from a 470 nm LED into the other end of the optical fiber. It should be noted that in comparison to 'standard' flat tip design (such as using a cleaved optical fiber) the taper enhances the power fraction of evanescent wave in the cladding and thus is sensitive to the changes in the local environmental, here resulting from the changes to the pH-sensitive coating[35].

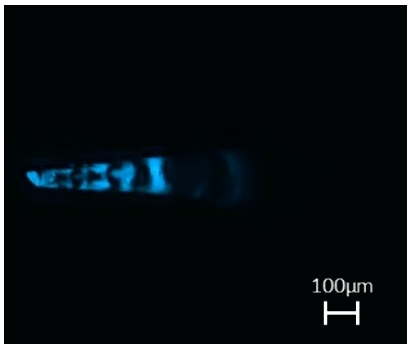

Figure 1 Image of a typical tip design when excited with a 470 nm LED.

The fluorescent monomer used (fluorescein O-methacrylate) was chosen since it is being appropriate for a detection range from pH 5.0 to pH 8.5 and it exhibits a strong luminescence signal. In addition, fluorescein O-methacrylate is polymerizable and it allows covalent binding to be used, in that way to overcome dye leaching problems[36]. Further, the fluorescein used acts as an indicator with the least negative charges compared to other indicator dyes (such as HPTS) and thus has a lower dependence on the ionic strength[23]. The mixture thus prepared, while in essence comparable to that shown in the literature[37], was importantly modified in such a way as to improve the coating process developed here.
To prepare this coating, 2-hydroxyethyl methacrylate (HEMA), the photo-initiator 4-(2-hydroxyethoxy)phenyl-(2-hydroxy-2-propyl)ketone (Irgacure 2959) used at 1.5%wt., 1,6-hexanediol diacrylate (HDDA) used at 5.0%wt. with respect to HEMA, the fluorescent monomer itself at 2.0%wt. with respect to HEMA and poly(ethylene glycol) diacrylate (PEGDA) at 3.0%wt to adjust the mechanical resistance, were fully mixed using a magnetic stirrer. To achieve this photo-polymerization, a simple process was used that took full advantage of the fiber-optic nature of the probe. The fiber tip was dipped into the prepared mixture and irradiated with light from a high power UV LED (365 nm peak wavelength, $P_0 \leq 500$mW) purchased from Omicron-Laserage GmbH. The irradiation time was optimized for this specific fiber design (and thus variated between 20 and 35 s) to create the polymerization of the material needed, and thus form repeatable and thin coatings on the fiber tips.

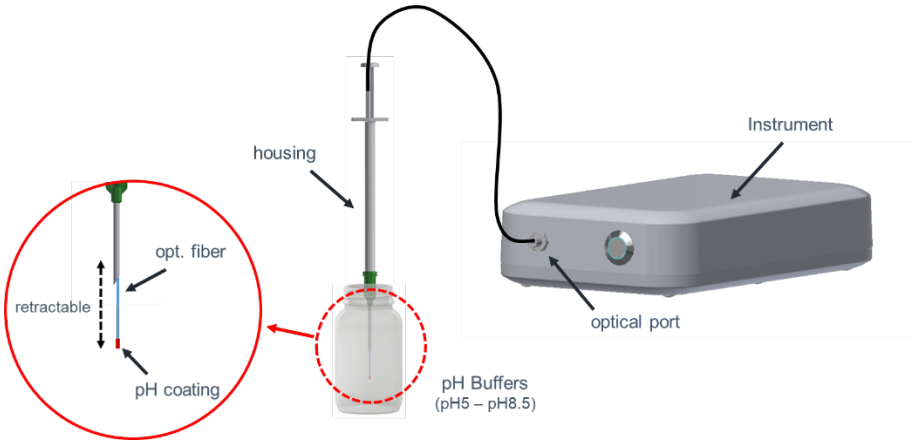

Figure 2 Illustration of the experimental setup and the fiber-optic sensor design with the new sensor tip and the pH sensitive layer attached (red). The optical fiber is protected in a retractable housing.

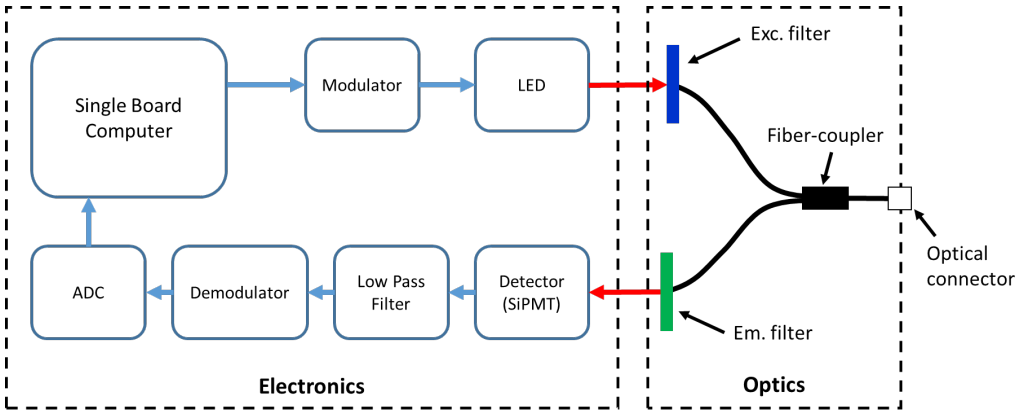

Figure 3 Block diagram of the instrument showing the main electronic and optical components.

Figure 2 shows an illustration of the fiber-optic sensor system designed and thus developed in this research. A simple but effective feature is that for simplicity and to reduce cost, the fiber-optic sensor itself was protected in a retractable housing, based on the design of a syringe. The inert housing and the small-sized tip (Ø < 50 µm) created specifically for this work make it ideal for biomedical and physiological applications. Here, often only small sample volumes are available for the measurement and thus many current commercial systems are not suitable.

Experimental set-up and methods

For the characterization of the pH sensors developed in this work a newly designed instrument was used with the specific purpose of monitoring the weak luminescence emission signals from the pH-sensitive coating attached to the fiber tip – in that way to give an accurate determination of the pH value. The instrument illustrated schematically in Figure 2, together with the main electronic and optical components, as shown in Figure 3, is important to minimize the effect of stray light so that it can work well with very low excitation intensities. This is critical for the high quality long-term performance sought, to reduce any photo-bleaching of the active element of the sensor, the indicator dye and maximize the sensor lifetime. To evaluate the device, each fiber-optic sensor was characterized by connecting it to the optical port and the output can then be monitored when the probe was dipped into five different pH buffers. Each of these measurements (at pH 5, pH 6, pH 7, pH 8 and pH 8.5) was performed under stable temperature and pressure and the pH values of the buffer solutions used were checked, both before and after each measurement, using a reference pH electrode as well as a temperature compensated fiber-optic sensing system (pH-1 micro and NTH-HP5) purchased from PreSens Precision Sensing GmbH to measure the temperature of the solution and thus allow correction of the pH values.

In the course of the experiment carried out to evaluate the system, first the relative intensity of the emission from the probe was measured in each buffer solution (in arbitrary units (a.u.)) and the system then calibrated using the Henderson-Hasselbalch equation (Eq. 3). The pH sensors were first dipped into the pH 7 buffer solution and then quickly (< 1s)

transferred to the pH8 buffer solution, to allow a measurement of the response time, Δt_{90}. A long-term drift in the sensor response was monitored when the probe was maintained in the pH 7 buffer solution over a 12h period, with a continuous irradiation of the sensor tip. This enabled a determination of any photo-bleaching arising from this extreme irradiation for 12 h.

The maximum temperature-induced pH change of the buffer solutions used has been determined by performing measurements at 25°C and 40°C, using the temperature compensated reference system. The effect of temperature on the sensor developed was investigated, over the range of 25°C to 40°C, by increasing the temperature of the buffer solutions (in steps of 5°C using a heating plate). In parallel, the temperature was monitored and controlled with the use of a Pt100 sensor and the pH value of the buffer solutions measured and corrected using the reference system. For each temperature and pH value, the relative intensity from the sensor was determined by averaging the signals over a time interval of 3 minutes. Further, the temperature-dependent sensor drift (arising from any photobleaching) has been investigated at pH7 and pH8 in buffer solutions using different sampling intervals (on-off phase of the excitation light source) of 1 s (continuous irradiation) and 5 s (t_{on} = 1 sec t_{off} = 4 sec.).

Experimental results and discussion

Optical and spectral properties

Since a fluorescein-based monomer dye was used as the pH sensitive indicator, the sensor reflects this in having a maximum absorbance at 490 nm and a peak emission wavelength at 520 nm[38]. Figure 4 shows the emission spectrum of the sensor tip. This choice of excitation light was based on creating an efficient separation of excitation and emission light, achieved through using a 470 nm LED with an optical filter to excite the sensor tip, where the emission light was detected through a suitable bandpass filter. This has the advantage of reducing the effect of stray light to a minimum, exploiting both the optical effects here and signal processing, making the system suitable for use in the bright environments where most measurements are needed.

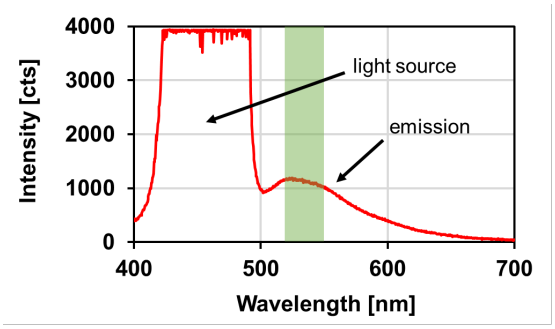

Figure 4 Emission spectrum (in the spectral range ~500 to ~700 nm) of the sensor tip when excited with light from a ~470 nm LED (seen from the saturated signal over the spectral range between ~400 and ~500 nm). The green area represents the approximate range of the emission filter.

Calibration and sensor response

The sensor developed exhibited an increase in fluorescence intensity with increasing pH values over the range studied. Figure 5 shows the steady state signal intensities obtained from the fiber-optic pH sensor when immersed in the range of different buffer solutions used. For each pH value, the relative intensity was determined by averaging the signals over a time interval of 10 s.

The dashed line in Figure 5 represents the fitted titration curve, applying Equation (3) with pK_a = 8.22 ± 0.07. The experimentally determined pK_a value is slightly higher than that reported for a comparable sensing film in the literature (pK_a = 7.9)[37]. However, the pK_a value of luminescence indicators varies, depending on its environment[39] and this can shift to a higher value when immobilizing an indicator into different polymers, due to a change in the polarity of the microenvironment[34].

The equation used describes the experimental results with a high level of precision (with a high correlation coefficient, R_2 = 0.999) and further tests carried out show that the calibrated pH sensors have a good repeatability as well as a comparable behaviour for decreasing pH values. The evaluation undertaken shows a sensor accuracy of approximately ±0.04 pH units (at pH 7) – using a conventional glass pH electrode as reference standard for simplicity. Figure 6 shows the changes in pH measured over the range from pH 5 to pH 8.5, for a calibrated sensor, showing a maximum signal variation (which is equivalent to < 0.01 pH units) and obtained for pH values greater than pH 6. An excellent signal-to-noise ratio has been obtained from the new sensor system design, exploiting in this way the very thin probe coating used, coupled to the electronic signal processing forming the instrument.

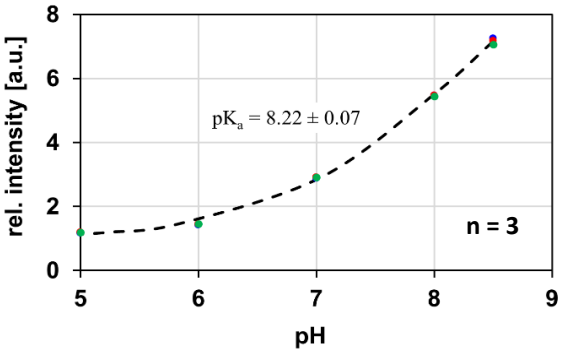

Figure 5 pH dependence of the luminescence intensity recorded over the range from pH 5 - pH 8.5 (and reproducible when measured three times). The dashed curve represents the fit using Equation (3) with R_2 = 0.999 and pK_a = 8.22 ± 0.07.

The rapid response time of the newly developed pH sensor has been studied in some detail, as shown in Figure 7, emphasizing this important feature of its operation. The sensor was shown to have a very fast response to pH changes, of Δt_{90} < 5s (with the period of ~1s taken to move the sensor physically from one buffer solution to another also included in that measurement),

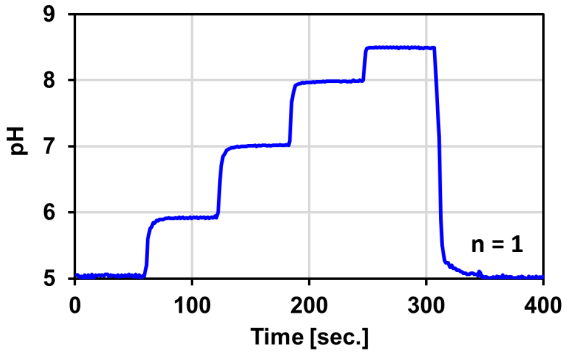

Figure 6 Measured pH changes in aqueous buffer solutions after calibration, stepping over the range pH 5 to pH 8.5 and illustrating the rapid response of the probe.

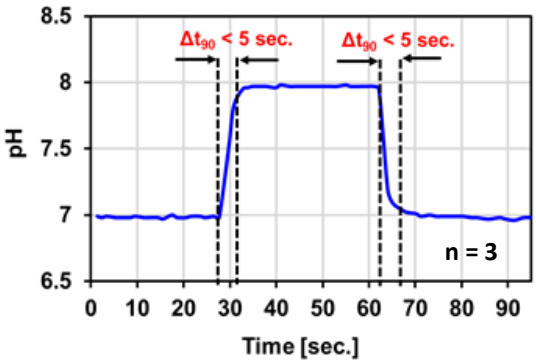

Figure 7 Response time of pH sensor probe due to a rapid (~1s) transfer from pH 7 to pH 8 and back to pH7, showing the average values and response time of the probe, $\Delta t_{90} < 5$s, when repeating this experiment three times (n=3).

and studied over the range from pH 7 to pH 8, and back to pH7. In this latter case (monitoring at pH 8), the sensor needed an additional 10s to reach the steady state, which was surprising as this phenomenon was not observed for the other sensor designs studied. It could therefore be assumed that this 'rogue result' was related to an inhomogeneous layer distribution and irregular thickness on the fiber tip that influences the pH changes locally. However, this overall very low, and importantly very fast response time is an unusual but very positive feature of the sensor design, when compared to the data published on a wide range of pH sensors described in the literature.

Moreover, the response time depends on the initial and final pH value: for pH values below pH 7 the response time was slightly slower; however, this was faster for pH values >pH 8.

Long-term stability and photostability

Figure 8 shows a continuous measurement made in a stable buffer solution (pH 7), for an extended period of ~12h, subjecting the probe to continuous irradiation to examine if any signal drift occurred and if there was evidence of photo-bleaching. It was pleasing to note that the pH sensor probe was very stable when compared to what is seen in the literature (with the drift being < 2.42 %/h), even though the determination of pH is based on a luminescence intensity measurement.

For this worst-case scenario (continuous irradiation and a sampling rate of 1 s) and for many applications where a sensor drift error of < 0.05 pH/h is acceptable, a re-calibration of the sensor would then be required after 3600 data points. This represents an extreme situation – and one which would not be seen in practice – as the probe would rarely be used with continuous irradiation for such a period. In a typical measurement situation, the duty cycle would be set with longer 'off-phases' of the excitation light source.

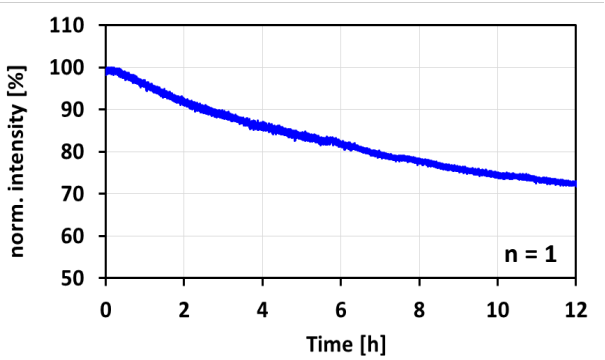

Figure 8 Luminescence signal decrease seen under continuous irradiation for ~12 h of the probe placed in a buffer solution of pH 7. The initial measurement (at t = 0) is 7.0 ± 0.05 with an average measured drift in the probe response over that period shown to be < 2.42 %/h – equivalent to a sensor drift error of < 0.05 pH/h.

Effect of temperature

Figure 9 shows the temperature-induced pH changes of the buffer solutions by comparing the measured pH value at 25°C and 40°C. The buffer solutions show a very good stability over the temperature range used in this work and were slightly increased at 40°C for pH values between pH5 and pH8 (ΔpH < 0.02) – only the pH8 buffer showed a maximum offset of ΔpH < 0.2. However, to investigate the temperature effect on the pH sensor, pH values were measured and corrected during all the temperature-based experiments carried out.

Figure 10 shows results obtained on the temperature 'cross-talk' of the pH sensor, monitoring over the physiologically important temperature range between 25°C and 40°C (in steps of 5°C). The results obtained showed that the sensor

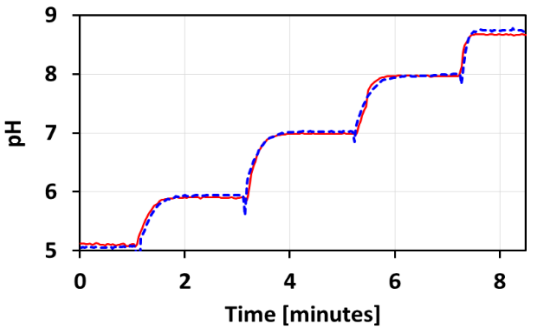

Figure 9 Measured pH values of the buffer solutions at 25°C (red) and 40°C (blue, dashed) using the temperature-compensated reference instrument.

performance showed no significant influence with temperature changes for pH values below pH 8. However, the calibration function starts to change at higher temperatures and for pH values greater the point of inflection (pK_a value of the indicator dye). The pK_a value is a thermodynamic parameter and therefore dependent on temperature changes[13] and this typically results in a linear shift of the overall calibration curve[10,40]. In addition, the deviation of pH (shown in Figure 11) for the overall detection range between pH 5 and pH 8.5 increases for higher temperature values, when compared to 'reference values' (here determined at 25°C).

However, temperature exerts somewhat complex effects on pH-sensitive materials and influences other parameters such as the swelling ratio of the hydrogel[41], and in the case here of the luminescence-based sensor developed, the thermal quenching of the luminescence of the indicator[13]. Further experiments carried out show that the decrease of luminescence emissions for pH values ≥ pH 8 seem mainly to be influenced by a higher bleaching rate of the indicator, seen at higher temperatures. Figure 12 shows the normalized emission signals of the sensor, determined at pH 8 and at a temperature, T, of 25°C. The signals were measured over ~20 minutes and data points were recorded with different 'on-off-phases' of the excitation light source whereas for a sampling interval of 1 s (red), the sensor tip was continuously irradiated and for a sampling interval of 5 s (blue), 'off-phases' of 4 s were added. As expected and due to a reduced light exposure of the pH sensitive material, no significant signal drift was measured for a sampling interval of 5 s, while a signal drift of ~0.1 %/minute occurred for continuous irradiation of the sensor. However, repeating this experiment at a temperature of 40°C (as seen in Figure 13), the results clearly show an increased signal drift for both the sampling intervals used here and thus this confirms a higher bleaching rate of the indicator in pH 8 and at 40°C. Comparing the results in Figure 11, the signal drift for a sampling interval of 5 s is significantly lower (~0.09 %/minute compared to ~0.23 %/minute) and this thus offers an efficient method to increase the long-term stability of the sensor when measurements above room temperature are required (important in biomedical applications). The results obtained and show here are very promising and already show a very high temperature stability of the sensor, especially for pH values < pH 8, which is unusual (when compared to other data published). In addition, it can be noted that no temperature compensation is required when performing precise pH measurements, in the temperature region between 25°C and 40°C, with the sensor developed in this work. However, further work is on-going to investigate how other parameters, such as the change in pk_a and the swelling ratio of the hydrogel, affect the temperature 'cross-talk' of the sensor.

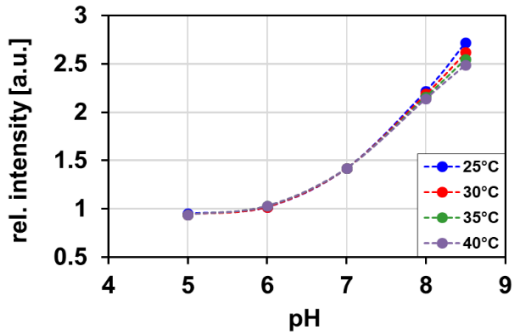

Figure 10 Effect of temperature on the calibration curve of the pH sensor for the physiological important temperature range between 25°C and 40°C.

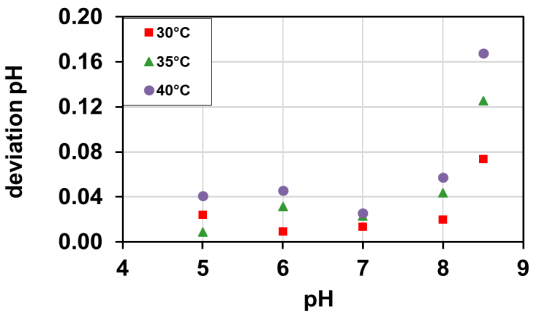

Figure 11 Temperature induced deviation of pH compared to a reference at a temperature of 25°C.

Mechanical stability

A mechanically stable sensor is important for many industrial uses and Figure 14 shows the result of a measurement made when the sensor was left in solutions of pH 6, pH 7 and pH 8 (buffer solutions) and to assess its mechanical stability under strong vibrations, in this case generated with a commercial ultrasonic cleaner. This device was turned on after 1 minute and turned off after 16 minutes (red), to examine whether a signal drift due to detachment of the coating or any damage to the tip occurs. The hydrogel-based coating shows an excellent adhesion to the glass surface and even under strong vibration, the small fiber tip was seen to be very stable mechanically – no damage could be seen when the tip was examined under a microscope. For pH 6 and pH 7, the graph shows a small signal increase after turning on the ultrasonic cleaner, but this decreases over time, when it is turned off again. This signal change is minor, not significant in the greater scheme of

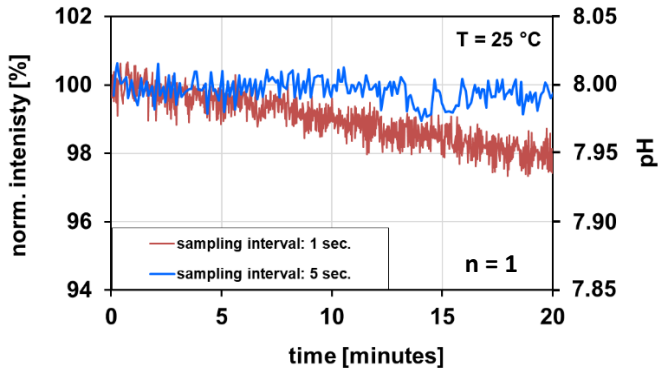

Figure 12 Normalized luminescence emission determined over 20 minutes in pH 8 and at T = 25°C. Signals measured with a sampling interval of 1 s (red) and 5 s (blue).

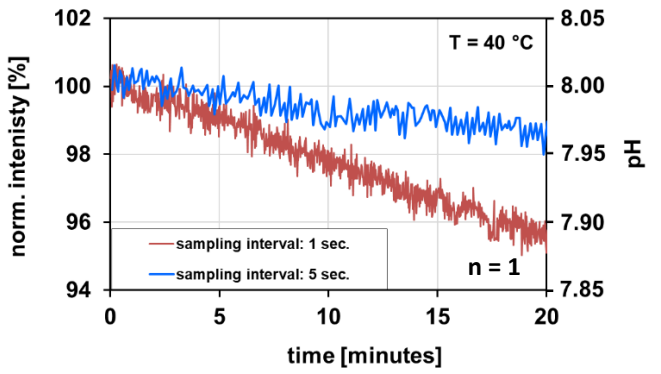

Figure 13 Normalized luminescence emission determined over 20 minutes in pH 8 and at T = 40°C. Signals measured with a sampling interval of 1 s (red) and 5 s (blue).

measurement but can be explained by the change of temperature from 25°C to 38°C in the buffer solution that arose from the ultrasonic irradiation of the sample. However, only at pH 8 does the signal decrease after the ultrasonic cleaner is turned on. This can be explained by the higher bleaching rate of the indicator, seen at higher temperatures, and shown (at 40°C) in Figure 13.

Taking this into account, it is clear that the results obtained show the excellent mechanical stability of the overall sensor design and emphasize its usability, even in harsh environments or flow systems where the sensor tip is mechanically stressed. In addition, the probe is shown to be immune to any effects of ultrasonic irradiation.

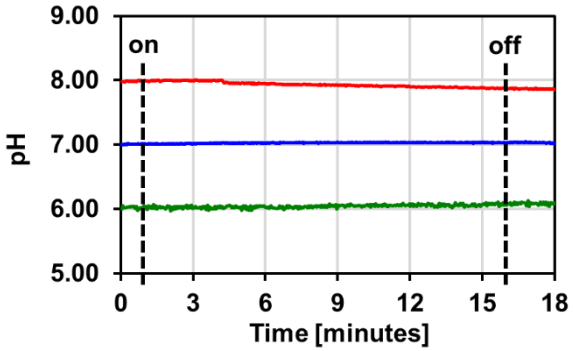

Figure 14 Mechanical stability of the sensor design measured in pH6 (green), pH7 (blue) and pH8 (red) solutions and under strong vibrations. An ultrasonic cleaner provided the vibration effect, by being turned on after 1 minute and off after 16 minutes (black, dashed).

Cross-comparison and illustrative measurement in a typical biological application

This final experimental section shows a cross-comparison of the pH-monitoring instrument developed in this work, with the output from a commercially available fiber-optic pH sensing system. To do so, results of a small-scale measurement in a biological application (using an AMES' medium) are shown, noting that these compare favourably with the performance seen from the commercial reference system.

Cross-comparison with other pH probe and instrument

Figure 15 shows a cross-comparison of the performance of the pH instrument developed in this work (blue) with that from a commercially available fiber-optic pH system (red) – one that has a comparable detection range (from pH 5.5 to pH 8.5). Each fiber-optic sensor was calibrated individually, then dipped into four different pH buffers (pH 5, pH 6, pH 7 and pH 8) and signals were monitored under constant environmental conditions (stable temperature and pressure).

With a response time of $\Delta t_{90} < 75$s, the commercially available pH sensor has a significant slower response time seen over the entire detection range. Further, the pH sensor developed in this work shows to have a better precision at value ~pH 7 (~6.96 pH compared to ~7.11 pH) and a slightly better signal-to-noise ratio for pH values >pH 6. This makes this sensing system very well suited to biomedical applications where both a high accuracy and small size of the sensor probe are required.

Experiment in a test-chamber for retinal studies

To provide an initial evaluation of the usability, accuracy and stability of the pH probe developed in this work for long-term measurements in this representative biological application, a simple experiment was carried out where the sensor was integrated in a test-chamber designed for retinal studies. The aim was to monitor the pH value in an AMES' medium close to the tissue – this being a substance which is important to maintain the metabolism of retinal cells and thus keeping these active.

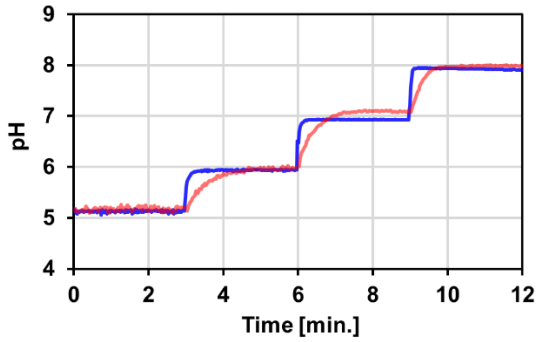

Figure 15 Cross-comparison of the pH sensor developed in this work (blue) with a commercially available sensor (red) stepping over the range pH 5 to pH 8.

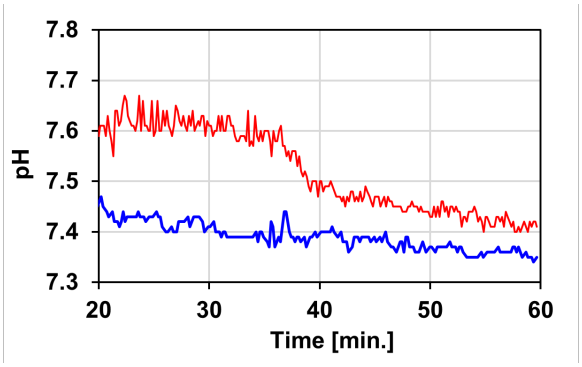

Figure 16 Results of a preliminary study to evaluate the performance of the sensor system for pH measurement in an AMES' medium for retinal studies – with the main experiment started at ~20 minutes after the system was inserted into the medium. The line in blue shows the response of the pH system developed in this work and red the data from a reference fiber-optic pH system used for comparison.

The AMES' medium used in this research was specially designed for these specific cell types and is both very well established, as well as being commercially available. (Further details of the AMES' medium are beyond the scope of this paper – a typical formulation as well as the preparation is described in the manufacturer's literature[42]). Before the experiment was undertaken, the pH value of the AMES' solution was adjusted to the optimal pH range for this study (between pH 7.4 and pH 7.5) using 1N HCL or 1N NaOH[42]. During the measurement process carried out, the AMES' medium passed through the test-chamber at a constant volume flow rate of 3 ml/min while its pH was measured over a period of 40 minutes, with the pH monitoring instrumentation developed in this work. To provide a comparison, a commercially available fiber-optic pH sensor was used as a reference.

The results obtained from this small-scale test are shown in Figure 16, revealing that the pH monitor developed in this work shows a better precision to the adjusted pH value of the AMES' medium (initial pH value between pH 7.4 and 7.5) while with the reference system a greater pH offset was measured. Unexpectedly, only the reference system shows a significant signal drop between 36 and 40 minutes, a phenomenon that might result from locally induced pH changes due to the volume flow of the AMES' medium or the pH sensor itself. (This phenomenon is not fully explained as yet and will be studied in further experiments). However, it could be a first indication that the new fiber-optic pH sensor developed has a better stability in a flow system than the conventional device and thus would be much more suitable for experiments of this type. In addition, the new pH-sensor shows a lower signal drift during the entire measurement process, which confirms the excellent photostability and mechanical stability discussed earlier.

As it is recognized that this evaluation is a 'proof of principle' of the sensor system: in further studies a more detailed and extensive investigation will be carried out. In such work, a pH regulation system would be implemented by automatically fumigating the AMES' medium with Carbogen (CO_2-bicarbonate) to allow better control of the pH level, achieving between pH 7.4 and pH 7.5. Thus it could be expected that the much faster response time of the newly developed pH sensor demonstrated here will show its major advantage when rapid pH changes occur. This is the subject of on-going evaluation work.

Conclusions

A new design of fiber optic-based pH sensor probe system has been developed, allowing the investigation of its system characteristics based on a new, fast response tip which has been created. The system has been evaluated as discussed and preliminary results reported are highly promising and show a significant improvement in the sensor performance on many current devices, with an extremely fast response time to pH changes ($\Delta t_{90} < 5s$). A key advantage is that with this new sensor design, very small volumes of solution can be used while results can still be highly accurate, because of the design involving small diameter optical fibers and small tip diameters. The work has prioritized monitoring of small volume samples, which often are the only ones available from biological or clinical work. In combination with the newly developed signal processing instrumentation used, the pH sensors created have been shown to be very stable over a long period of time – during a

measurement for 12 hours at pH 7 with continuous irradiation, a low signal drift (of less than 2.42 %/h) and a negligible influence of stray light were observed. Figure 8 shows the change in the reading with long, continuous irradiation and this signal drift could be reduced or eliminated by changing the duty cycle used, with longer 'off phases' of the excitation light source.

On-going R&D work planned will continue to optimize the sensor further, including to study and optimize the thickness of the sensor layers (but maintaining the positive trade-off between the layer thickness and the response time), as well as evaluate in more detail and thus reduce or eliminate any cross sensitivities to other parameters (e.g. ionic strength).

A very positive conclusion of the study carried out is that it has clearly shown that this new sensor design has the potential to extend the breadth of applications for fiber-optic pH sensors, taking full advantage of the fast response times seen from this design. As has been shown in a cross-comparison with a commercially available fiber-optic pH sensor, the sensor developed in this works has a higher precision and significant faster response times to pH changes. Further, in a small-scale biological experiment reported, the pH value in an AMES' medium for retinal tissue can readily be monitored during a long-term measurement. It is recognized that additional experiments of this type are needed and further, the detection range of the pH sensors is ideal for measurements in biotechnical applications, where a pH range from pH 5 to pH 8.5 is necessary and small sensors are needed. A further benefit of this design for biological or clinical applications is that the manufacturing process for these sensors is relatively simple and thus volume production, at low cost, is feasible – creating an approach which will also suit a range of applications including those where easy and inexpensive disposal of the sensor probe is required after each use.

Acknowledgements

The authors wish to acknowledge Alexander Schäfer for the great support in software development and Claudia Ingensiep from University Hospital of Aachen for performing the experiments in their test-chamber for retinal studies. Grattan and Sun acknowledge support from the Royal Academy of Engineering.

References

1 J. Werner, M. Belz, K.-F. Klein, T. Sun and K.T.V. Grattan, *Measurement*, 2021, 109323.

2 D. Wencel, A. Kaworek, T. Abel, V. Efremov, A. Bradford, D. Carthy, G. Coady, R. C. N. McMorrow and C. McDonagh, *Small (Weinheim an der Bergstrasse, Germany)*, 2018, **14**, e1803627.

3 S. Chen, Q. Yang, H. Xiao, H. Shi and Y. Ma, *Sensors and Actuators B: Chemical*, 2017, **241**, 398–405.

4 Q. Yang, H. Wang, S. Chen, X. Lan, H. Xiao, H. Shi and Y. Ma, *Analytical chemistry*, 2015, **87**, 7171–7179.

5 P. O'Mara, A. Farrell, J. Bones and K. Twomey, *Talanta*, 2018, **176**, 130–139.

6 P. Gruber, M. P. C. Marques, N. Szita and T. Mayr, *Lab on a chip*, 2017, **17**, 2693–2712.

7 S. A. Mousavi Shaegh, F. de Ferrari, Y. S. Zhang, M. Nabavinia, N. Binth Mohammad, J. Ryan, A. Pourmand, E. Laukaitis, R. Banan Sadeghian, A. Nadhman, S. R. Shin, A. S. Nezhad, A. Khademhosseini and M. R. Dokmeci, *Biomicrofluidics*, 2016, **10**, 44111.

8 A. S. Jeevarajan, S. Vani, T. D. Taylor and M. M. Anderson, *Biotechnology and bioengineering*, 2002, **78**, 467–472.

9 Y. Kostov, P. Harms, L. Randers-Eichhorn and G. Rao, *Biotechnol. Bioeng.*, 2001, **72**, 346–352.

10 C. Staudinger, M. Strobl, J. P. Fischer, R. Thar, T. Mayr, D. Aigner, B. J. Müller, B. Müller, P. Lehner, G. Mistlberger, E. Fritzsche, J. Ehgartner, P. W. Zach, J. S. Clarke, F. Geißler, A. Mutzberg, J. D. Müller, E. P. Achterberg, S. M. Borisov and I. Klimant, *Limnol. Oceanogr. Methods*, 2018, **16**, 459–473.

11 C. R. Schröder, B. M. Weidgans and I. Klimant, *The Analyst*, 2005, **130**, 907–916.

12 T. H. Nguyen, T. Venugopala, S. Chen, T. Sun, K. T.V. Grattan, S. E. Taylor, P. M. Basheer and A. E. Long, *Sensors and Actuators B: Chemical*, 2014, **191**, 498–507.

13 A. Steinegger, O. S. Wolfbeis and S. M. Borisov, *Chemical reviews*, 2020, **120**, 12357–12489.

14 C. G. Frankær, K. J. Hussain, T. C. Dörge and T. J. Sørensen, *ACS sensors*, 2019, **4**, 26–31.

15 PyroScience GmbH, *AquapHOx.* Underwater Oxygen Sensors. Datasheet, available at: https://www.pyroscience.com/en/applications/applications/underwater-solution, accessed 24 November 2020.

16 PyroScience GmbH, *PHROBSC-PK6.* Robust pH Screw Cap Probe. Datasheet, available at: https://www.pyroscience.com/en/products/all-sensors/phrobsc-pk6#Downloads, accessed 24 November 2020.

17 PreSens Precision Sensing GmbH, *PM-HP5.* pH Microsensor, available at: https://www.presens.de/products/detail/profiling-ph-microsensor-pm-hp5, accessed 24 November 2020.

18 U. Kosch, I. Klimant and O. S. Wolfbeis, *Fresenius' Journal of Analytical Chemistry*, 1999, **364**, 48–53.

19 X.-d. Wang and O. S. Wolfbeis, *Analytical chemistry*, 2013, **85**, 487–508.

20 X.-d. Wang and O. S. Wolfbeis, *Analytical chemistry*, 2016, **88**, 203–227.

21 X.-d. Wang and O. S. Wolfbeis, *Analytical chemistry*, 2020, **92**, 397–430.

22 D. Wencel, T. Abel and C. McDonagh, *Analytical chemistry*, 2014, **86**, 15–29.

23 B. M. Weidgans, Universität Regensburg, 2004.

24 T. Jokic, S. M. Borisov, R. Saf, D. A. Nielsen, M. Kühl and I. Klimant, *Analytical chemistry*, 2012, **84**, 6723–6730.

25 M. Strobl, T. Rappitsch, S. M. Borisov, T. Mayr and I. Klimant, *Analyst*, 2015, **140**, 7150–7153.
26 A. Richter, G. Paschew, S. Klatt, J. Lienig, K.-F. Arndt and H.-J. P. Adler, *Sensors (Basel, Switzerland)*, 2008, **8**, 561–581.
27 I. Klimant, C. Huber, G. Liebsch, G. Neurauter, A. Stangelmayer and O. S. Wolfbeis, in *New Trends in Fluorescence Spectroscopy*, ed. O. Wolfbeis, B. Valeur and J.-C. Brochon, Springer Berlin Heidelberg, Berlin, Heidelberg, 2001, vol. 1, pp. 257–274.
28 *United States Pat.*, US6602716B1, 1998.
29 F. Mohamad, M. G. Tanner, D. Choudhury, T. R. Choudhary, H. A. C. Wood, K. Harrington and M. Bradley, *The Analyst*, 2017, **142**, 3569–3572.
30 C. McDonagh, C. S. Burke and B. D. MacCraith, *Chemical reviews*, 2008, **108**, 400–422.
31 Arne Wilhelm Zimmer, Philipp Raithel, Mathias Belz, Karl-Friedrich Klein, *in Proc. SPIE 9886-34*, 2016.
32 K.-F. Klein, C.P. Gonschior, X.Ruan, M.Bloos, G.Hillrichs, H.Poisel, *Proc. 18th POF-conference*, 2009.
33 S. P. L. Sørensen, in *Biochem. Zeit.*, vol. 21, pp. 131–304.
34 A. S. Vasylevska, A. A. Karasyov, S. M. Borisov and C. Krause, *Analytical and bioanalytical chemistry*, 2007, **387**, 2131–2141.
35 S. Guo and S. Albin, *Optics express*, 2003, **11**, 215–223.
36 A. M. Breul, M. D. Hager and U. S. Schubert, *Chemical Society reviews*, 2013, **42**, 5366–5407.
37 L. Rovati, S. Cattini, P. Fabbri and L. Ferrari, in *2018 International Flexible Electronics Technology Conference (IFETC)*, IEEE, 2018 - 2018, pp. 1–5.
38 N. Klonis and W. H. Sawyer, *Journal of fluorescence*, 1996, **6**, 147–157.
39 L. D. Lavis, T. J. Rutkoski and R. T. Raines, *Anal. Chem.*, 2007, **79**, 6775–6782.
40 C. Staudinger, M. Strobl, J. Breininger, I. Klimant and S. M. Borisov, *Sensors and Actuators B: Chemical*, 2019, **282**, 204–217.
41 H. van der Linden and J. Westerweel, in *Encyclopedia of Microfluidics and Nanofluidics*, ed. D. Li, Springer US, Boston, MA, 2013, pp. 1–5.
42 Sigma-Aldrich Chemie GmbH, *Product Information Sheet: AMES' Medium,* available at: https://www.sigmaaldrich.com/content/dam/sigma-aldrich/docs/Sigma/Product_Information_Sheet/1/a1420pis.pdf, accessed 10 February 2021.